# SOME DESIGN FEATURES OF THE 80 MEV H⁻ ISOCHRONOUS CYCLOTRON IN GATCHINA

G.Riabov, S.Artamonov, E.Ivanov, G.Mikheev, B.Tokarev, Yu.Mironov, Petersburg Nuclear Physics Institute, S-Petersburg, Russia
P.Bogdanov, V.Mudrolubov, NIIEFA, S-Petersburg, Russia

*Abstract*

The history of the design and costruction of the 80 MeV H⁻ isochronous cyclotron as well as some design features are discribed.

## INTRODUCTION

The cyclotron complex is designed for fundamental and applied researches – production of medical isotopes, beam therapy of eye melanoma and surface types of cancer. Besides the cyclotron is to be used as injector for C-230 synchrotron which is planed to be built for proton therapy of cancer diseases of human internal organs utilizing the Bragg peak.

To minimize the expenditures while designing the cyclotron an attempt was made to use at most the existing synchrocyclotron infrastructure, i.e. building, the bridge crane for 30 ton, electric power, water cooling, ventilation system etc. The iron yoke of the existing synchrocyclotron magnet model is used for the magnet system.

Acceleration of H⁻ ions has obvious advantages: possibility for 100% extraction of the beam with high intensity and variable energy. On the other hand it requires special source of H⁻ ions, high vacuum and what is most important magnetic field strength in the magnet sector should not exceed in our case 17 kGs to prevent H⁻ electromagnetic dissociation.

Design and construction of H⁻ isochronous cyclotron have been in progress for many years and by the year 2010 design and drawings for the main accelerator subsystems had been completed [1,2,3]. The cyclotron magnet was designed, produced, commissioned and put into operation, full scale magnetic measurements were begun. The main problem by that time became purchase of industrially and commercially produced equipment that was realized in the frame of the nuclear medicine program of National Research Centre Kurchatov Institute. Starting from September of 2010 the cyclotron and beam transport line equipment is mounted in experimental hall.

## GENERAL DESCRIBTION

Main parameters of the cyclotron are presented in Table 1. The detailed information about cyclotron equipment is presented in the report on this conference.

## FEATURES OF THE MAGNETIC SYSTEM

In addition to the standard cyclotron for H⁻ machine there is an additional and essential requirement - to keep H⁻ losses on dissociation below than 5%.

### *H⁻ Losses and the Magnetic Structure*

Two alternative versions of the magnetic structures have been examined. The first one (1) have flutter F = 0.04, spiral angle γ =55°, harmonic amplitude A4 = 4.15 kGs and the second one (2) have F = 0.025, γ = 65°, A4 = 3.28 kGs on the final radius. Here γ is an angle between the radius vector at radius r and tangent to the median line of sectors at the same radius. Both modifications provide about the same net axial focusing and differ by the field in the hill region. Fig. l. presents the beam losses due to electromagnetic dissociation for two versions of the magnetic structures. The second version - with low flutter and high spiral angle was selected for Gatchina cyclotron since it provides beam losses below than 5%.

Table 1: Main parameters of the cyclotron

| | |
|---|---|
| **MAGNET** | |
| Pole diameter | 2.05 m |
| Valley gap | 386 mm |
| Hill gap (min) | 164 mm |
| Number of sectors | 4 |
| Spiral angle (max) | 65 degrees |
| Isochronous filed in the center | 1.352 T |
| Flatter (max) | 0.025 |
| Ampere- turns | $3.4\times 10^5$ |
| Power | 120 kW |
| Weight | 250 t |
| **HF. SYSTEM** | |
| Frequency | 41.2 MHz |
| Potential | 60 kV |
| Harmonics | 2 |
| HF power | 2×40 kW |
| **VACUUM** | |
| Pressure | $10^{-7}$ tor |
| 2 cryogenic pumps | 2×3500 l/s |
| 1 turmomolecular | ($H_2$) |
| **H⁻ source** | |
| Multipole | 1.5 mA |
| Injection energy | 26 kV |
| **AXIAL INJECTION** | |
| Transport system: solenoid lens, solenoid, inflector | |
| **EXTRACTION SYSTEM** | |
| Stripping method | |
| Energy range | 40-80 MeV |

### *Magnetic Structure with High Spiral Angle*

Parameters of the C-80 magnetic structure are presented in table 1. Fig.2 presents top view of the pole tips of the magnetic system

ISBN 978-3-95450-125-0



Copyright © 2012 by the respective authors — cc Creative Commons Attribution 3.0 (CC BY 3.0)

With use of the Novosibirsk MERMAID code which accounts for iron saturation and permit to use up to $20\times10^6$ nodes the profile of the iron shims was determined. Details are discussed in special poster report at this conference.

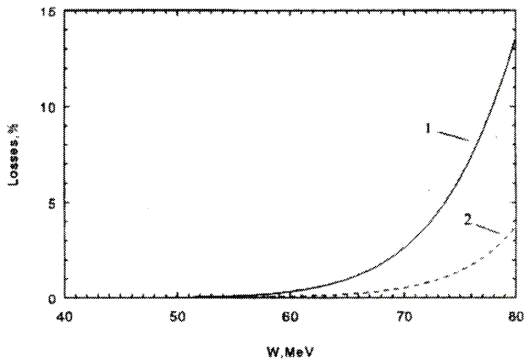


Figure 1: $H^-$ losses due to electromagnetic dissociation for two magnetic structures.

Distribution of the magnetic field in the full scale magnet was measured using the measuring system based on twenty NMR calibrated Hall probes and automated coordinate system which can position probes in cylindrical coordinate system with accuracy of 0.1 mm along the radius and azimuth at the radius of 100 cm. Achieved precision was equal to $2\times10^{-4}$ with total time of measurements of 6-8 hours. Disagreement between experimental measurements and calculations did not exceed 20 Gs. Final distribution of the magnetic field was measured experimentally with 2-5 Gs precision.

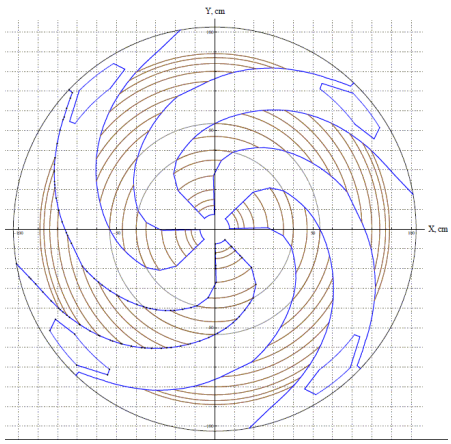


Figure 2: Top view of the pole tip.

## *Flutter versus Radius for Straight Sectors*

The valley and hill gaps have been estimated by using the calculation of the flatter in straight sector structure. Flatter versus radius is presented in Figure 3 for two variants of magnetic structures. The comparison of the different magnetic structures is performed by using a non-dimensional parameter $x = r/N{\cdot}g_h$, where $g_h$ and $g_v$ denote half of hill and valley gaps, N=4 is number of sectors, azimuthally lengths of valley and hill are equal.

Flutter increases when the hill gap is decreased and decreases with growth of sector number. For the case of $x < 0.5$ that corresponds to the range of radii $r < 0.5\cdot Ng_h$ the value of flutter rapidly decreases. In our case at radii smaller than two gaps in the hill the edge focusing became ineffective.

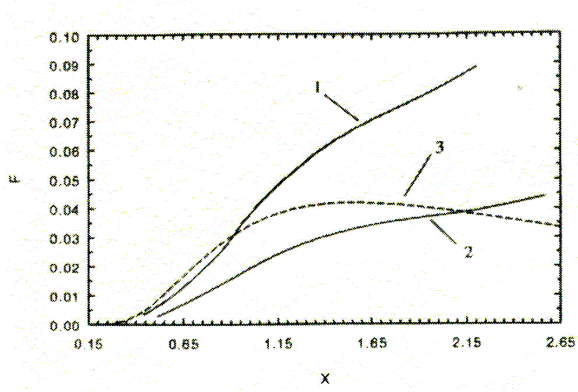


Figure3: Flutter as a function of the non-dimensional parameter:

1. $2g_v = 386$ mm, $2g_h = 170$ mm, $h_1 = 108$ mm;
2. $2g_v = 284$ mm, $2g_h = 145$ mm, $h_2 = 69$ mm;
3. Approximation of the sector uniform magnetization for the case 1.

## *Effect of Spiral Pole Tips*

Spiral angle provides extra focusing due to angular focusing. Effectively flutter is increased by the following factor:

$$S(r, \gamma) = 1 + 2\tan^2\gamma(r),$$

where $\gamma(r)$ is a spiral angle at given radius. However in real life benefit in focusing is smaller than it could be expected from this expression. It is explained by the drop of flutter at small radii and difference between spiral angle for pole tips and magnetic field. Drop of flutter due to introduction of spiral angle can be understood based on simple geometrical considerations [4]. Influence of spiral angle on flutter value can be estimated from calculation of flutter for a straight sector (see Fig.4) if one makes the following replacement: $x_{eff} = x\cos\gamma$.

The total effect from spiral angle can be characterized with parameter which is a product of flutter F and $S(r,\gamma)$. Since value of flutter rapidly decreases at $x_{eff} < 0.5$ than introduction of spiral angle can result in decreased focusing. For each value of radius and parameter x there is a critical spiral angle that results in increase of focusing from introduction of spiral angle. The value of critical angle for each value of x can be found as a square root of:

$$U(x,\gamma) = (F(x\cos\gamma)/F(x))\cdot(1+2\tan^2\gamma) - 1 = 0,$$

where $F(x)$ is a function similar to one shown in Fig. 3. For the spiral angles more than critical one for the given

Copyright © 2012 by the respective authors — cc Creative Commons Attribution 3.0 (CC BY 3.0)

ISBN 978-3-95450-125-0

radius the introducing of the spirally decreases the vertical focusing.

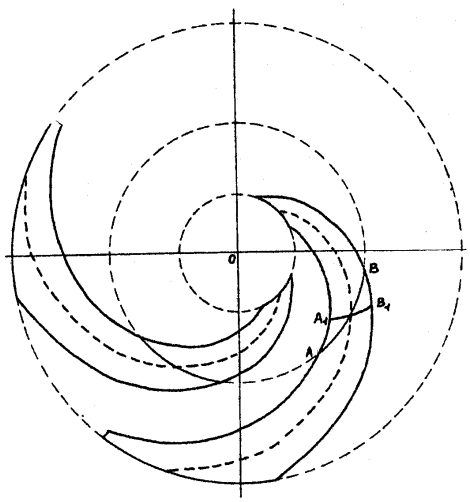


Figure 4: Difference between the sector length along azimuth and "effective" length at large spiral angle. AB-length of sector along azimuth. $A_1B_1 \approx AB \cdot \cos\gamma$ – effective width of sector along perpendicular to the middle line.

Fig.5 shows critical spiral angle in dependence on radius for our accelerator. According to the plot spiral angle becomes ineffective at radii r < 15 cm and structure with high spiral angle is advantages at r > 35cm. In the central region is necessary to use the straight sector structure.

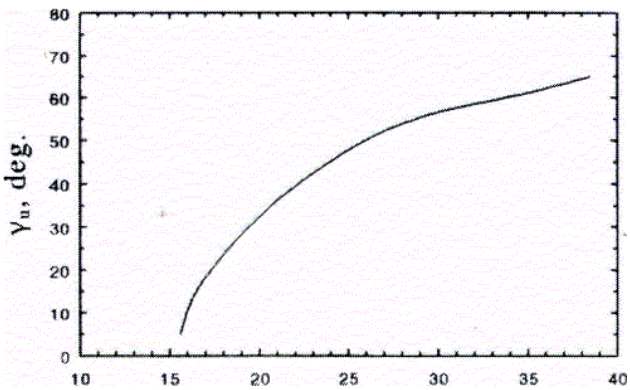


Figure 5: The ultimate spiral angle in dependence on radius for $2g_v$ = 386mm, $2g_h$ = 170mm, r = N·$g_h$ ·$x_{eff}$,, N=4.

## VACUUM CHAMBER, INJECTION, EXTRACTION AND EXPERIMENTAL AREA

The external ion source and axial injection are used to obtain high vacuum for the acceleration $H^-$ ions. Moreover in the adopted design magnetic system is placed outside of the chamber of the accelerator. The upper and lower lids of the chamber are attached to the poles of a magnet. Thus, to improve the vacuum conditions, two walls of the chamber (2 × 16 mm) occupy about 10% of the magnet gap, which required an increase in ampere-turns and the power of the magnet.

The extraction with 100% efficiency of high intensity beam and energy variation from 40 up to 80 MeV is realized by H- stripping methods. The schematic view of the extraction system is presented in Figure 6.

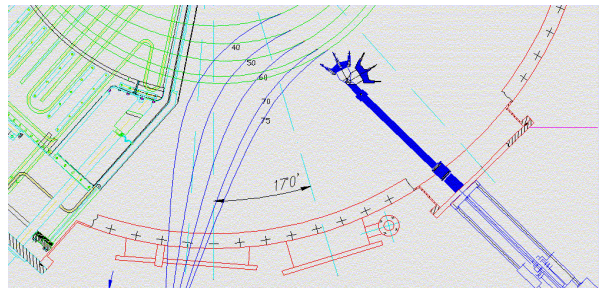


Figure 6: Schematic view of the extraction system.

For more details about extraction system of the cyclotron please refer to the poster presentation at this conference.

The multy-purpose experimental complex consists of the targets of different specialization and the beam transport lines. A beam of high intensity is transported to the basement, where three stationary targets are installed for production of medical radioisotopes and pharmaceutical medications as it shown in Figure 7.

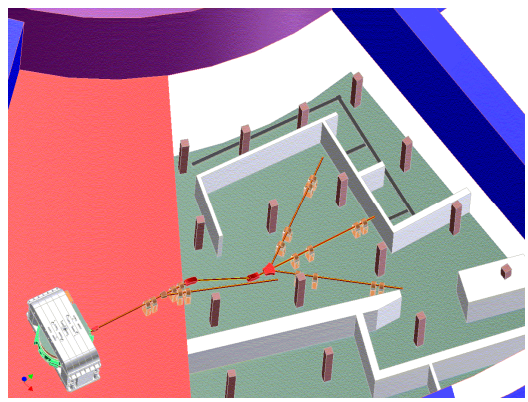

Figure 7: Transport lines to the targets for production of medical radioisotopes.

On the ground floor are disposed the ophthalmology facility with low intensity beam line, centre for radiation testing of electronics components and transport line for the injection in the new medical synchrotron.

## REFERENCES

[1] N.K. Abrossimov et al. Proc. XIII Intern. Conf. on Cycl. and their Applic., Vancouver, Canada 1992, p.. 54-62
[2] N.K. Abrossimov et al. RUPAC-XIII , Russia, Dubna, 1993, v.2, p. 205-209
[3] N.K. Abrossimov et al. RUPAC-XIV , Russia, Protvino, 1994, v.4, p. 5-10
[4] N.K. Abrossimov et al. . Proc. XV Intern. Conf. on Cycl. and their Applic., Caen, France 1997, p.. 58-62

ISBN 978-3-95450-125-0



Copyright © 2012 by the respective authors — cc Creative Commons Attribution 3.0 (CC BY 3.0)